



The role of grain boundary energy in grain boundary complexion transitions



Gregory S. Rohrer

Department of Materials Science and Engineering, Carnegie Mellon University, 5000 Forbes Ave., Pittsburgh, PA 15213-3890, USA

ARTICLE INFO

Article history:

Received 23 November 2015
Revised 5 March 2016
Accepted 13 March 2016
Available online 16 March 2016

Keywords:

Grain boundaries
Grain boundary energy
Complexions
Microstructure
Grain boundary thermal grooves

ABSTRACT

Recent findings about the role of the grain boundary energy in complexion transitions are reviewed. Grain boundary energy distributions are most commonly evaluated using measurements of grain boundary thermal grooves. The measurements demonstrate that when a stable high temperature complexion co-exists with a metastable low temperature complexion, the stable complexion has a lower energy. It has also been found that the changes in the grain boundary energy lead to changes in the grain boundary character distribution. Finally, recent experimental observations are consistent with the theoretical prediction that higher energy grain boundaries transform at lower temperatures than relatively lower energy grain boundaries. To better control microstructures developed through grain growth, it is necessary to learn more about the mechanism and kinetics of complexion transitions.

© 2016 Elsevier Ltd. All rights reserved.

1. Introduction

The characteristic structure and chemical composition of a grain boundary [1], free surface [2], phase boundary [3], or dislocation [4] are referred to as its complexion. Extensive research has shown that grain boundary complexions can abruptly transition from one state to another in response to a change in composition or temperature [5,6]. These transitions are thought to occur because they reduce the grain boundary excess free energy [7]. The purpose of this paper is to review recent findings on the role of the grain boundary energy in complexion transitions. Efforts to measure the change in grain boundary energy associated with a complexion transition will be reviewed and the role of the anisotropy of the grain boundary energy will be discussed. Because the experiments have mostly explored the changes in complexion that occur as a function of temperature, we will begin by reviewing what is known about the effect of temperature on the grain boundary energy. Next, experimental methods to measure the change in energy will be described and the results of those measurements will be reviewed. Experiments probing the influence of grain boundary energy anisotropy will then be discussed and, in the final section, some of the most important directions for future research will be outlined.

2. Temperature dependence of the grain boundary free energy

The grain boundary free energy of a pure material is expected to decrease linearly with increasing temperature because of the entropic term in the free energy. Measurements of pure Ni and Cu, among other materials, are consistent with this expectation [8–10]. For example, in the temperature range between 600 and 1000 °C, the grain boundary energy of Cu decreases by 0.4 J/m² and in the temperature range between 800 and 1400 °C, the grain boundary energy of Ni decreases by 0.1 J/m² [9]. Atomistic simulations can be used to calculate the temperature dependence of the grain boundary energy and these results also show that the energy decreases with temperature [11–16]. However, the decrease in energy is not perfectly linear, especially at temperatures near absolute zero and close to the melting point [13]. Over this range, Foiles [13] determined that the grain boundary energy of Ni decreases from 1.2 J/m² at 0 K to 0.4 J/m² at the melting point. For comparison, the surface energy of Cu decreases about 25% from room temperature to the melting point [12]. The evidence from both the experiments and the calculations suggest that the decrease in the grain boundary energy of pure materials is continuous.

In a system with impurities or alloying components, the situation is expected to be different. In most cases, the solute will accumulate at the grain boundaries and reduce the grain boundary energy. As temperature increases, the bulk solubility usually increases; if the solute from the intergranular regions dissolves in the bulk, the boundary excess will be reduced, and this will increase the grain boundary free energy. This general idea has been

E-mail address: rohrer@cmu.edu

used to interpret a large amount of alloy data that shows grain boundary energies increase with temperature. For example, the grain boundary energies of Cu alloys with ≤ 1 atomic percent Zr, Te, Ti, or Cr increases by 0.035 J/m^2 (Zr) to 0.065 J/m^2 (Cr) between 700 and 900 °C [8,9]. Measurements of Ga–Pb alloys have shown that surfaces behave in a similar way, with the surface energy increasing as the surface excess decreases at higher temperatures [17]. In other words, the increases in grain boundary energy driven by the change in boundary composition more than compensate for the entropic factor that tends to reduce the grain boundary energy. Changes in the grain boundary energy that occur because of the de-segregation of solute from the boundaries at high temperature are thought to be continuous, at least until the solute is depleted and the entropic effect prevails.

If the solute content of a boundary is metastable, and it transitions to a stable composition, then there can be a discontinuous change in the grain boundary composition and this might lead to a discontinuous change in energy. For example, in yttria doped alumina, it has been observed that increases in Y content (or decreases in the total grain boundary area from grain growth) lead to increased grain boundary excess of Y [18]. The grain boundary excess reaches a maximum of 9 Y/nm^2 and then, at higher concentrations, yttrium aluminum garnet (YAG) precipitates form and the grain boundary excess decreases to a value that remains constant ($6\text{--}7 \text{ Y/nm}^2$) with an increased concentration of Y. This decrease in Y excess at the boundaries would presumably lead to an abrupt increase in the grain boundary energy. If a Y-doped alumina ceramic supersaturated in Y is heated, then at the temperature that YAG precipitates, one might also expect an abrupt lowering of the grain boundary excess and a corresponding increase in the grain boundary energy.

Precipitation of a second phase is one mechanism that can occur to partition excess solute in the microstructure, but it is now known that transitions to thicker grain boundary complexions (carrying more solute) are also possible. If, as temperature changes, one grain

boundary complexion becomes more stable than another, then the rate of change of the grain boundary energy with temperature will also change (see Fig. 1(d)) [7,19,20]. If the boundary remains in a metastable state at a higher temperature, then, when the boundary ultimately transforms, there will be a discontinuous change in the energy. Phase boundaries likely behave in a similar way, and it has been shown that the formation of an interface complexion at a gold-sapphire interface reduces the interface energy [3].

The four possible scenarios for the change in the grain boundary energy with temperature, at constant bulk composition, are illustrated in Fig. 1. Note that they lead to characteristic differences in the temperature dependence; continuous negative (a) or positive (b) slopes indicate that the temperature dependence is driven by entropic effects or impurity de-segregation, respectively. Both of these cases have been observed experimentally [9]. An abrupt increase in grain boundary energy, as illustrated in Fig. 1(c), is expected to occur if precipitates form and the boundaries are depleted of solute. To the author's knowledge, no reports illustrating this effect on the grain boundary energy have been reported. If there is a complexion transition, then the temperature dependence of the grain boundary energy will change slope [7,19,20]. If the transition must be activated, and the higher energy complexion exists in a metastable state until sufficiently super heated, then there will be an abrupt decrease in the grain boundary energy, as indicated in Fig. 1(d). These characteristically different phenomena make it possible to distinguish between precipitation and a complexion transition and this is the basis for some of the experiments described Section 4 [21–27].

3. Grain boundary energy measurements

Experimental grain boundary energy measurements are usually carried out by observing the geometry of interface junctions assumed to be in thermodynamic equilibrium [28]. In this context, we will consider grain boundary thermal grooves that form when a

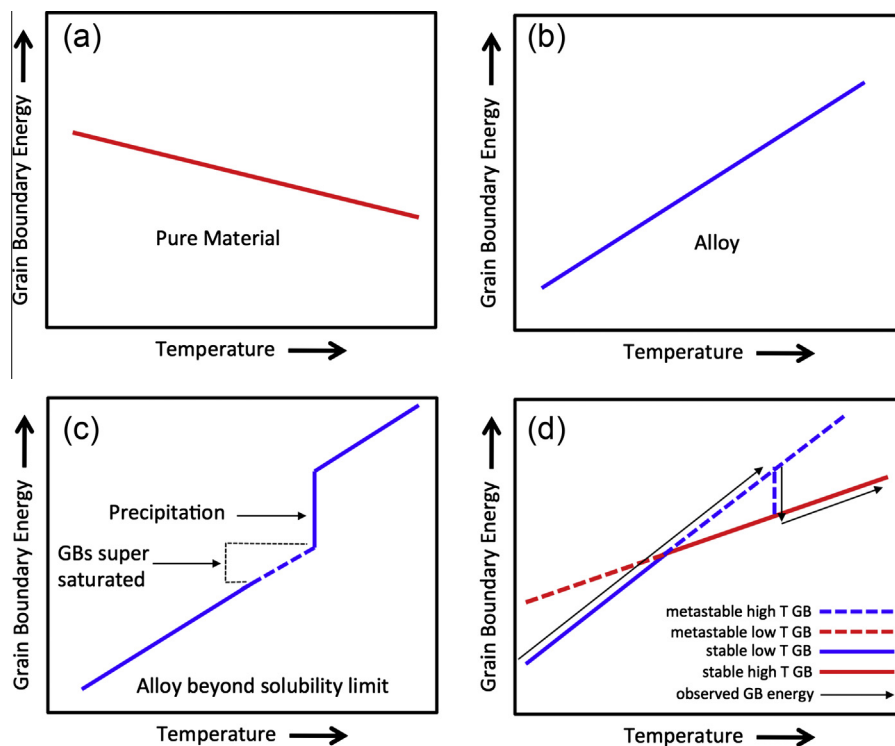


Fig. 1. Schematic depictions of how the average grain boundary energy can vary with temperature in (a) a pure material, (b) an alloy with segregating solute, (c) an alloy where the solubility limit is exceeded, and (d) a material with multiple grain boundary complexions.

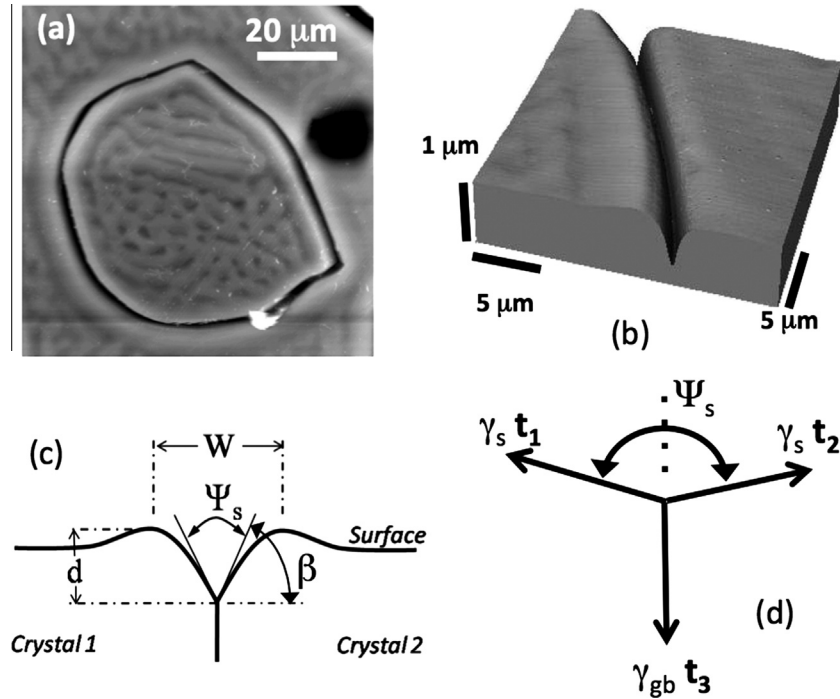


Fig. 2. (a) AFM image of the thermal groove at a closed loop grain boundary in SrTiO₃ [31]. (b) Section of the thermal groove in (a), illustrated in three dimensions. (c) Profile of the thermal groove, defining the geometric parameters used in Eqs. (1) and (2). (d) The balance of interfacial forces used to determine Eq. (1) [31].

grain boundary meets a free surface [29]. Atomic force microscopy (AFM) is a relatively simple way to observe groove shapes, as illustrated in Fig. 2. A simplification of the Herring [30] equilibrium condition for triple junctions leads to an equation that makes it possible to measure the grain boundary to surface energy ratio (γ_{gb}/γ_s) based on the geometry of the thermal groove (defined in Fig. 2):

$$\gamma_{gb}/\gamma_s = 2 \sin \beta = 2 \cos(\Psi_s/2) \quad (1)$$

Furthermore, the theory of thermal grooving [29] makes it possible to determine the appropriate geometric parameters from measurements of the groove width and height:

$$\tan \beta = 4.73(d/W) \quad (2)$$

The parameters used in Eqs. (1) and (2) are defined in Fig. 2.

In practical measurements of the relative grain boundary energy, it is necessary to consider the finite size of the probe compared to the actual groove dimensions. Consideration of these factors has led to the conclusion that if the grooves are wide enough ($W > 1 \mu\text{m}$), the finite probe size should not affect the measurement and, for narrower grooves, a correction can be applied [32]. It should also be noted that Eq. (2) is increasingly less accurate for large values of β . However, the errors are known and this makes it possible to correct the data [33]. Finally, there are a number of approximations in Eq. (1) that must be considered when applying it to measurements. First, it is assumed that the two surface energies on either side of the groove root are the same and this is, in general, not true. Second, it is assumed that the grain boundary is normal to the surface plane and, again, this is not true in general. Third, it is assumed that the differentials of the surface and grain boundary energy with respect to orientation are small enough to be ignored and this is, again, not true [34,35]. Because of these approximations, the measurement of a single grain boundary groove has little meaning. Therefore, the approach that has been adopted is to measure many grooves and examine the distribution

of values of γ_{gb}/γ_s , which samples variations in the unknown parameters listed above. Using observations of more than one hundred grooves, it has been shown that the mean value and width of the distribution are reproducible characteristics of the sample [32].

4. Relationships between grain boundary energy and grain boundary complexion

4.1. Grain boundary energy changes resulting from complexion transitions

The earliest work examining the relationship between grain boundary complexion transitions and grain boundary energy considered doped alumina ceramics [25]. Based on the earlier work of Dillon and Harmer [6,36–38], it was assumed that grain boundaries around large, abnormal grains had a high mobility complexion and that boundaries around the smaller grains had the low mobility complexion (see Fig. 3). In other words, abnormally large grains were used as indicators for boundaries that had transformed and it was assumed that the boundaries around the smaller grains were metastable with respect to the high mobility complexion, at least at the annealing temperature. Relying on this assumption, one must recognize that it is possible that not every boundary surrounding the large grain has transitioned to the high mobility complexion. Further, boundaries around the smaller grains might have transitioned, but did not create an abnormally large grain either because not enough time elapsed for the grain to increase in size to differentiate it from the others, or not enough of the boundaries surrounding that grain had transformed and allowed it to grow abnormally large.

To evaluate the energy difference between boundaries that had transformed and those that did not, Dillon et al. [25] used thermal groove measurements to compare the distribution of γ_{gb}/γ_s for boundaries on abnormal grains (type-1 in Fig. 3) and boundaries neighboring abnormal grains (type-2 in Fig. 3). An example of

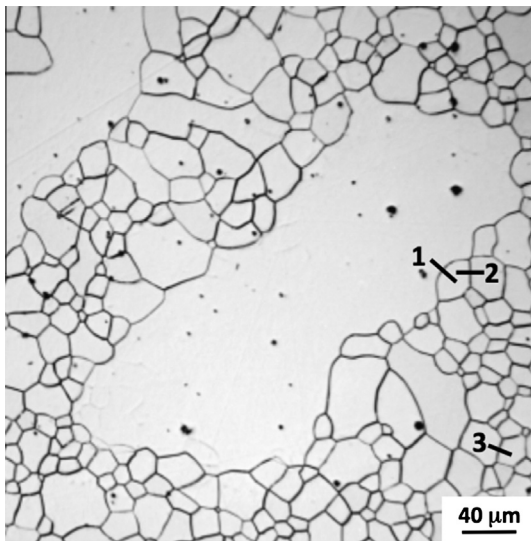


Fig. 3. Optical micrograph of an alumina microstructure with a bimodal grain size distribution. It is assumed that high mobility grain boundaries around the large grains co-exist with metastable low mobility grain boundaries around the smaller grains. The labels 1, 2, and 3, signify examples of boundaries that are around an abnormally large grain (1), neighboring a large grain (2), and far from a large grain (3) [25].

the results for 100 ppm Nd-doped alumina, annealed at 1400 °C, is illustrated in Fig. 4. While the distributions overlap, there is also a clear difference in the median values of γ_{gb}/γ_s . In this case, the energies of the boundaries around the large grains, assumed to have transformed to the high mobility complexion, have energies that are (on average) 16% lower than those around the smaller grains. Interpreting this with respect to Fig. 1(d), this is the energy difference between the metastable low temperature complexion (dashed line) and the stable high temperature complexion (solid line). Because we cannot be certain that all of the type-1 boundaries were transformed and that all of the type-2 boundaries were not transformed, the result has to be accepted as an estimate of the difference. It should be kept in mind that this is an average measure; each grain boundary energy is expected to be slightly

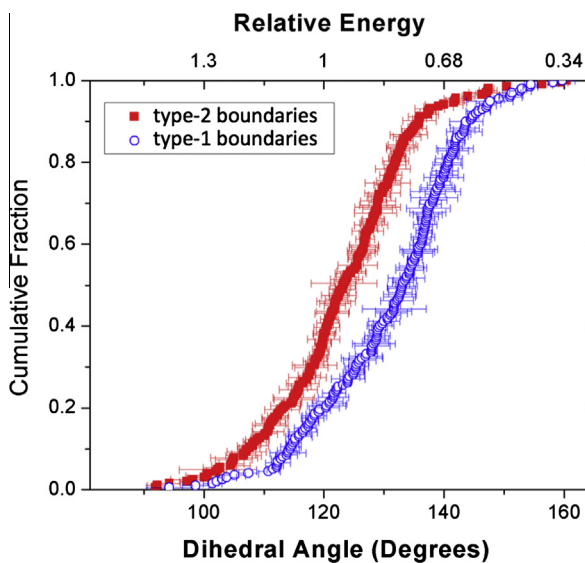


Fig. 4. Comparison of the relative grain boundary energies of type-1 (bounding abnormally large grains) and type-2 (bounding normal grains) grain boundaries in 100 ppm Nd-doped alumina annealed at 1400 °C [25].

different and its energy change when it transforms is also potentially different.

The experiment described above for Nd-doped alumina was repeated for several other materials with the following results [25]. For 100 ppm Y-doped alumina at 1400 °C, the decrease was 46%, for 500 ppm Mg-doped alumina at 1700 °C, the decrease was 26%, for 30 ppm Ca-doped alumina at 1200 °C, the decrease was 20%, and for 200 ppm Si-doped alumina at 1200 °C, the decrease was 10%. In each case, the interpretation is that the stable complexion around the abnormally large grains has a reduced energy compared to the metastable complexion around the smaller grains. There were, however, three examples that did not show a decrease in energy: 30 ppm Ca-doped alumina at 1400 °C, 200 ppm Si-doped alumina at 1400 °C, and 200 ppm Si-doped alumina at 1750 °C. While there are several feasible explanations for this result, a later study of Ca-doped yttria suggests that it may be a problem with the assumption that type-2 boundaries are not transformed, as described below.

Grain boundary energy measurements, similar to those described above, were carried out on 100 ppm Ca-doped yttria annealed at 1700 °C for 6 h, at which point abnormally large grains co-exist with much smaller grains (see Fig. 5(b)) [22,23]. In this case, the energies of type-1, -2, and -3, grain boundaries were compared to each other and to boundaries in a sample heated for a much shorter time that had no abnormally large grains. As in some of the cases above, the type-1 and type-2 boundaries had energy distributions that were indistinguishable, suggesting they have the same complexion. However, type-3 boundaries, several grain diameters away, had energies that were 40% larger and comparable to the boundaries in the sample with no abnormal grains. This suggests that both the boundaries around the abnormal grains and the boundaries nearby had transformed to the lower energy complexion and the boundaries further away remained in the metastable, high energy complexion. This might explain why, in some of the past studies that compared only the type-1 and type-2 boundaries, no energy difference were detected.

The observation that grain boundaries adjacent to large grains are more likely to have transformed to the more stable, low energy complexion than grains far from the abnormal grains may provide some information about the mechanism of the transformation and this was explored in a recent study using a mesoscale grain growth simulation [39]. The study used a three-dimensional Monte Carlo simulation to probe the links between possible complexion transition paths and the microstructures that result. One of the findings that is pertinent to the observations described above is that if individual grain boundaries transform randomly, then no one grain has enough high mobility grain boundaries to give it a sustained advantage over the others, and abnormal growth is not observed. The second important finding is that if one imposes the condition that boundaries connected to transformed boundaries through a triple line have a higher probability of transitioning than those not connected, then the transformed boundaries tend to cluster and abnormally large grains are observed. Assuming this mechanism is responsible for the formation of large grains with a persistent growth advantage, then one would expect the boundaries labeled type-2 here (adjacent to the large grains) to have energy distributions similar the type-1 boundaries around the large grains. While this is observed in some systems (such as 100 ppm Ca-doped yttria), other systems (such as 100 ppm Y-doped alumina) show distinct differences between the type-1 and type-2 boundaries.

Simulations have also shown that complexion transitions can reduce the grain boundary energy. For example, in simulations of $\Sigma 5$ (210) and (310) symmetric tilt grain boundaries in copper, structurally distinct complexions were detected that had energies that differed by 1–3% at 0 K [40]. The boundaries transform from

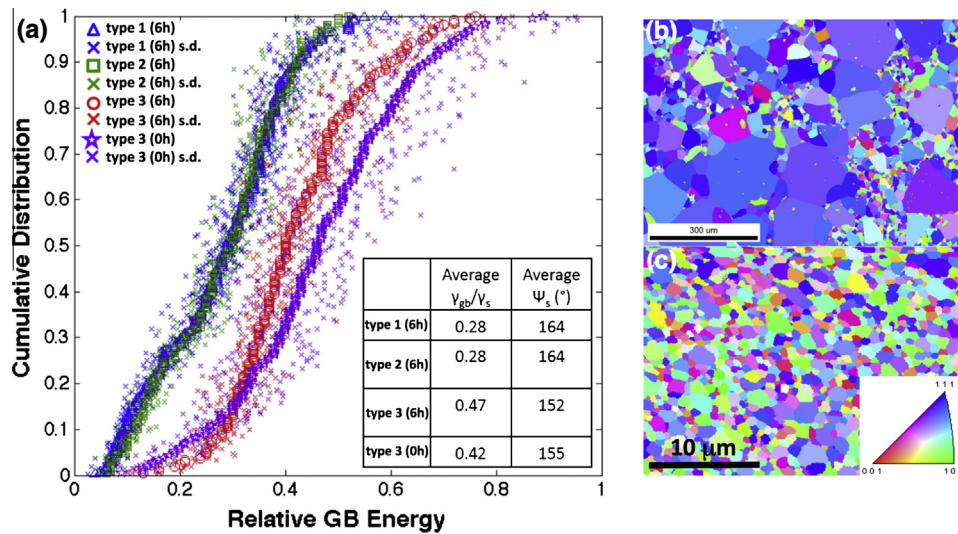


Fig. 5. Comparison of the relative grain boundary energies of different types of grain boundaries in 100 ppm Ca-doped yttria. The sample shown in (b) was heated for 6 h at 1700 °C and is labeled 6 h. The sample shown in (c) was heated to 1700 °C and then immediately quenched and is labeled 0 h. (a) Relative grain boundary energies determined from thermal grooves formed at 1300 °C for 30 min. The standard deviations (s.d.) of multiple measurements from the same groove are also marked. Note that distributions for type 1 (6 h) and type 2 (6 h) are indistinguishable and overlap. (b) EBSD orientation map of the 6 h sample and (c) EBSD orientation map of the 0 h sample [22].

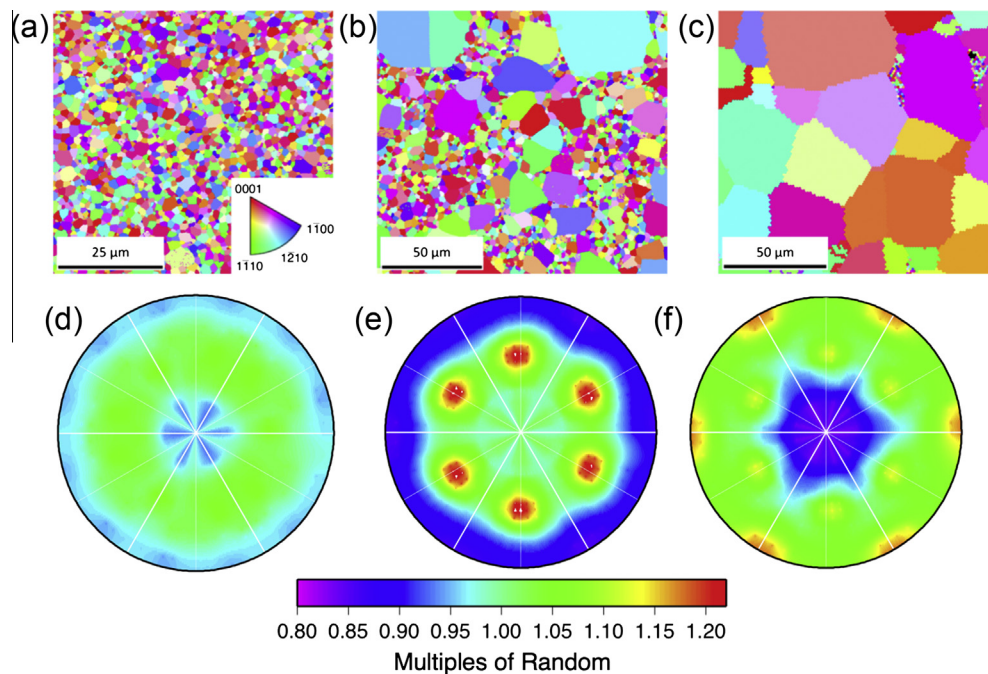


Fig. 6. (a–c) Orientation maps illustrating the microstructures and (d–f) grain boundary plane distributions for 450 ppm Y-doped alumina. (a and d) 1450 °C, (b and e) 1500 °C, (c and f) 1600 °C. The grain boundary plane distributions are plotted in stereographic projection with the [0001] direction normal to the page and the [1120] reaction horizontal [24].

the structure stable at low temperature to the one stable at higher temperatures in the range of 300–400 K. Near the melting point, the boundaries make a final transition to a liquid-like structure. Similar simulations of the $\Sigma 5$ (210) boundary in Cu with a small amount of Ag (0–4 atomic%) have shown a transition from a boundary with a monolayer of segregated Ag to a bilayer of segregated Ag. While this leads to a reduction in the energy, the energy reduction is again found to be very small, less than 0.1 mJ/m² [41]. A first principles study of the Ni–Bi system shows that for a $\Sigma 5$ (210) boundary in Ni, segregated Bi bilayers reduced the energy by about 13% and that both monolayers and trilayers were less stable [42]. In contrast, segregation of Bi to the low energy $\Sigma 3$ (111) boundary did not

lower the energy. These calculations are consistent with experimental observations showing bilayers of Bi at general Ni grain boundaries and no Bi at the $\Sigma 3$ (111) boundary [1].

4.2. Grain boundary character distribution and grain boundary complexions

There is an interplay between grain boundary complexions, the grain boundary energy distribution, and the types of grain boundaries found in the grain boundary network. Specifically, the grain boundary character distribution (GBCD), which is the relative areas of different types of grain boundaries, also changes when the grain

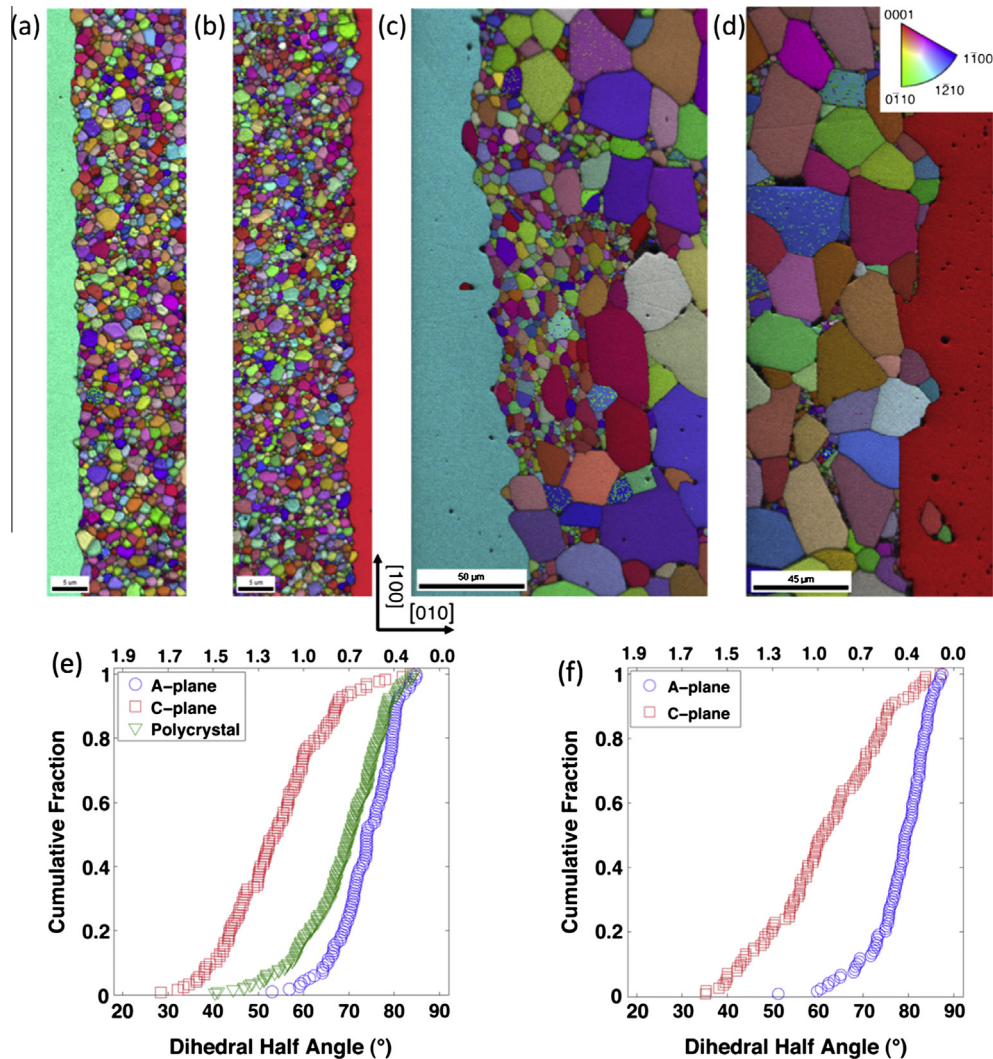


Fig. 7. (a–d) Orientation maps of cross-sections of the sandwich samples. (a) Near the interface with the (1120) plane and (b) near the (0001) plane in the as consolidated sample. (c) and (d) are also near the (1120) (c) and (0001) plane (d), respectively, but recorded after annealing at 1500 °C for 8 h. The lengths of the scale bars are (a) 5 μm, (b) 5 μm, (c) 50 μm, and (d) 45 μm. (e) Cumulative distributions of relative grain boundary energy for (e) the sample that was thermally grooved immediately after consolidation, (f) the sample annealing for 8-h at 1500 °C inducing AGG. Those labeled A-plane are grain boundaries including the (1120) single crystal, those labeled C-plane are grain boundaries including the (0001) single crystal, and those labeled polycrystal are grain boundaries touching neither of the single crystals [21].

boundary complexion changes [43,44]. It is now well established that grain boundary populations are distributed in a way that is inversely correlated to the grain boundary energy [28,45–47], so that when the energies change, so does the GBCD. For example, Fig. 6 shows the distribution of grain boundary planes (and examples of the microstructure) in 450 ppm Y-doped alumina after three different thermal treatments [24]. At 1450 °C, the grain size distribution is normal and the grain boundaries are presumed to be in the low temperature complexion (Fig. 6(a)). At 1500 °C, there is a bimodal grain size distribution and the coexistence of two complexions is assumed (Fig. 6(b)). Finally, at 1600 °C, the larger grains have impinged and the boundaries are now almost entirely the high temperature, low energy complexion (Fig. 6(c)). At the same time, there is a shift from a nearly isotropic grain boundary plane distribution (Fig. 6(d)), to one that is dominated by (1120) planes (Fig. 6(f)). We know that the population of grain boundaries is inversely related to the energy, so these results demonstrate that the energies of the grain boundaries do not change uniformly in a complexion transition, but some are more affected than others. In this example, boundaries terminated by (1120)-type planes are

lower in energy with respect to the other orientations. This same phenomenon has been observed in other materials [23,27].

4.3. Role of grain boundary energy anisotropy in complexion transitions

The observations discussed at the end of Section 4.1 for the Ni–Bi system illustrate the important effect of grain boundary energy anisotropy on complexion transitions. Specifically, at a single temperature and Bi-concentration, higher energy grain boundaries (such as $\Sigma 5$ (210)) transform to a complexion with a Bi bilayer and low energy boundaries (such as $\Sigma 3$ (111)) do not [1,42]. This is consistent with the original theories for complexion transitions that, at constant temperature, there is a critical energy below which boundaries would not transform and, above which, boundaries could undergo a transition to a lower energy complexion [48]. Experiments were recently conducted to determine how the grain boundary energy affected the nucleation of a complexion transition in Y-doped alumina [21]. The experiment used sandwich-like samples consisting of a doped alumina polycrystal

sandwiched between two single crystals of sapphire of known orientation. The orientations were selected so that one crystal that has a surface orientation associated with high energy boundaries, (0001), and the other has an orientation associated with low energy boundaries, (11 $\bar{2}$ 0). Therefore, distinct grain boundary energy distributions are created at the two single crystal–polycrystal interfaces and more of the boundaries at the low energy interface will be stable in the low temperature complexation than at the higher energy interface.

The results in Fig. 7 are consistent with this idea. The low and high energy sides of the sandwich sample, following consolidation at 1300 °C, are shown in Fig. 7(a) and (b), respectively. The grain boundary energy distributions, measured at the two interfaces are shown in Fig. 7(e). The (11 $\bar{2}$ 0) or A-plane has the lowest mean energy, the (0001) or C-plane has the highest mean energy, and random boundaries between the interfaces (labeled ‘polycrystal’) have intermediate energies. After annealing the sample at 1500 °C (Fig. 7(c) and (d)), it is clear that more large grains are present along the high energy interface (Fig. 7(d)) than along the low energy interface (Fig. 7(c)), consistent with the idea that the nucleation of the complexation transition is more likely to occur at high energy boundaries than low energy boundaries.

4.4. Competition between precipitation and complexation transitions

As suggested in Fig. 1(c) and (d), there are two possibilities for partitioning excess solute at grain boundaries. One is to precipitate the excess solute as a second phase, which is expected to deplete the boundaries of solute and increase the grain boundary energy. The other is to transform to a complexion that accommodates more solute at the boundary and this is expected to reduce the

grain boundary energy. The competition between these two processes should depend on the energetic barriers associated with reaching the final state. While very little is known about the barrier for complexation transitions, the activation barrier for the nucleation of a new phase is proportional to the cube of the interface energy between the matrix and parent phase and inversely proportional to the square of the free energy of formation of the phase. One can hypothesize that when this barrier is high, complexation transitions are more likely and when the barrier is low, precipitation is more likely.

To estimate the relative sizes of these barriers, the relative interface boundary energy was measured by the thermal grooving technique on samples where a parent phase was diffusion bonded to the precipitate phase, as illustrated in Fig. 8 [26]. The measurements were carried out for Mg-, Ca-, Y-, and Si-doped aluminas, and the results are summarized in Table 1. The materials with the highest barrier for the nucleation of a new phase have more complexation transitions and they occur at lower temperatures than those with low barriers to nucleation. The differences in the activation energy largely derive from the differences in the interface energies. These results suggest that interface energies should guide the selection of additives that will suppress or promote complexation transitions.

5. Challenges for the future

While there have been several recent authoritative reviews about wetting and complexation phenomena [5,49,50], the field is relatively young and there are still many things we do not know about grain boundary complexions. In fact, a better understanding of grain boundary complexions was recently stated as a grand chal-

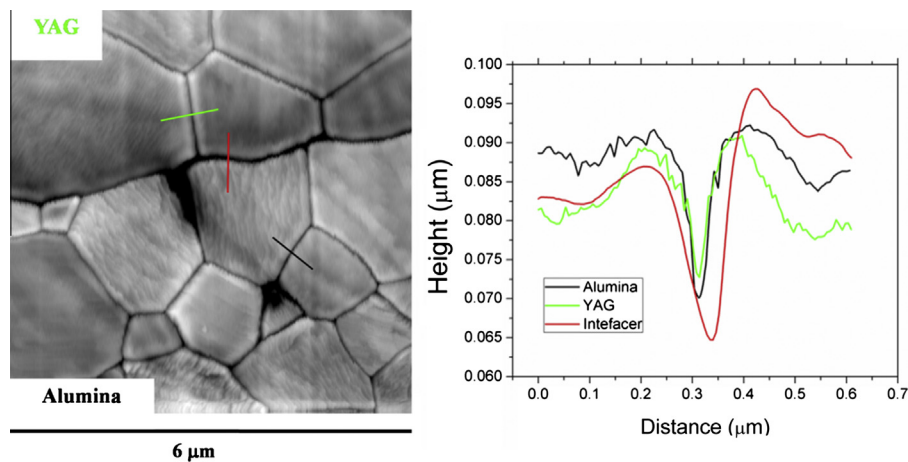


Fig. 8. AFM image of the interface between an yttrium aluminum garnet (YAG) polycrystal and an alumina polycrystal. The green, red, and black traces on the image show examples of thermal groove profiles for YAG, the interface, and alumina, respectively [26]. (For interpretation of the references to color in this figure legend, the reader is referred to the web version of this article.)

Table 1

A list of the relative interface to alumina grain boundary energy ratio, the temperature at which the onset of abnormal grain growth begins in the associated system, the number of complexation transitions that the system displays, and a factor representing the magnitude of the activation barrier that is the ratio of the relative interface energy cubed to the free energy of formation squared. The relative energies have arbitrary units, a.u. [26].

Phase (B)	$\gamma_{A/B}/\gamma_{G.B.}$	Onset of 1st transition	Number of complexions	$(\gamma_{A/B}/\gamma_{G.B.})^3/(\Delta G_f)^2 (\times 10^5)$, a.u.
Magnesium aluminate spinel	0.37	~1650 to 1750 °C	2	1.6
Calcium Hexaluminatate (basal)	0.51	~1550 to 1650 °C	3	2.4
Yttrium aluminum garnet	0.9	~1400 to 1500 °C	5	4.3
Silica	1.13	~1200 to 1300 °C	5	90
Calcium Hexaluminatate (non-basal)	1.5	~1200 to 1300 °C	5	42

lenge for the future of ceramic science [51] and advances in materials characterization should make it possible to meet that challenge [52]. The overarching challenge is to attain the ability to predict the occurrence of complexion transitions, in a way analogous to how we can predict the occurrence of bulk phases in temperature-composition space. To do this, one needs to understand both their thermodynamic basis and the kinetics of their transitions. One can argue that the thermodynamics of complexions are reasonably well established and, as a result, complexion diagrams, analogous to phase diagrams, are now being used to systematically represent the ranges of stability of different grain boundary complexions [5,53]. The kinetics of complexion transitions is only now beginning to be probed. The long range goal should be to establish time-temperature-transformation (TTT) diagrams for complexions [54].

There are a number of things that we do not know about the kinetics of complexion transitions. For a bulk phase, there is a critical temperature for the transformation. If there is a barrier to the transformation, then the stable and metastable phases can co-exist, at least temporarily. The same appears to be true for complexions, but there is a complicating factor. Each grain boundary with a distinct energy will have a different critical temperature for transformation. In other words, the points where the red and blue lines cross on Fig. 1(d) are different for each type of grain boundary. Therefore, multiple grain boundary complexions may be stable at a single temperature, but at boundaries with different energies. This seems to be confirmed by observations reported by Bojarski et al. [21], but it is also possible that there is a nucleation barrier for the transition. The conclusions from the simulations by Frazier et al. [39] suggest the stable complexion nucleates heterogeneously on boundaries that are connected through a triple line to a boundary that is already transformed.

While it is possible to experimentally map out TTT diagrams for grain boundary complexion transitions, the work would be greatly accelerated by a firm theoretical foundation and this will not be possible until the nucleation mechanism is understood. It is possible that the results of atomistic simulations or in situ high resolution microscopy will provide important clues to the mechanism. However, quantitative experiments comparing the actual transition rates to measured rates will be necessary to verify proposed mechanisms.

6. Conclusions

The grain boundary energy plays an important role in grain boundary complexion transitions. Experiments and computer simulations show that high temperature complexions have lower energies than the corresponding metastable low temperature complexion. The change in grain boundary energy causes a change in the grain boundary character distribution. There is also evidence that higher energy grain boundaries transform to the lower energy complexions at a lower temperature than low energy grain boundaries. To control microstructures with multiple co-existing complexions in a predictive way, it is necessary to better understand, at a theoretical and experiment level, the kinetics of complexion transitions; this should be a fruitful area for future research.

Acknowledgement

Financial support from the ONR-MURI under the Grant No. N00014-11-1-0678 is gratefully acknowledged.

References

- [1] J. Luo, H.K. Cheng, K.M. Asl, C.J. Kiely, M.P. Harmer, The role of a bilayer interfacial phase on liquid metal embrittlement, *Science* 333 (6050) (2011) 1730–1733, <http://dx.doi.org/10.1126/science.1208774>.
- [2] J. Luo, Y.-M. Chiang, Wetting and prewetting on ceramic surfaces, *Annu. Rev. Mater. Res.* 38 (2008) 227–249, <http://dx.doi.org/10.1146/annurev.matsci.38.060407.132431>.
- [3] M. Baram, D. Chatain, W.D. Kaplan, Nanometer-thick equilibrium films: the interface between thermodynamics and atomistics, *Science* 332 (6026) (2011) 206–209, <http://dx.doi.org/10.1126/science.1201596>.
- [4] M. Kuzmina, M. Herbig, D. Ponge, S. Sandloebes, D. Raabe, Linear complexions: confined chemical and structural states at dislocations, *Science* 349 (6252) (2015) 1080–1083, <http://dx.doi.org/10.1126/science.aab2633>.
- [5] P.R. Cantwell, M. Tang, S.J. Dillon, J. Luo, G.S. Rohrer, M.P. Harmer, Grain boundary complexions, *Acta Mater.* 62 (2014) 1–48, <http://dx.doi.org/10.1016/j.actamat.2013.07.037>.
- [6] S.J. Dillon, M. Tang, W.C. Carter, M.P. Harmer, Complexion: a new concept for kinetic engineering in materials science, *Acta Mater.* 55 (18) (2007) 6208–6218, <http://dx.doi.org/10.1016/j.actamat.2007.07.029>.
- [7] M. Tang, W.C. Carter, R.M. Cannon, Grain boundary transitions in binary alloys, *Phys. Rev. Lett.* 97 (7) (2006) 4, <http://dx.doi.org/10.1103/PhysRevLett.97.075502>.
- [8] G. Barreau, G. Brunel, G. Cizeron, P. Lacombe, Diffusion in copper-silver system – heterodiffusion and chemical diffusion – influence of low Cr, Te, Ti and Zr additions to copper, *Mem. Scient. Rev. Metall.* 68 (5) (1971) 357.
- [9] D. Gupta, Diffusion, solute segregations and interfacial energies in some material: an overview, *Interface Sci.* 11 (1) (2003) 7–20, <http://dx.doi.org/10.1023/a:1021570503733>.
- [10] W. Lange, A. Hassner, G. Mischer, Messung der korngrenzendiffusion von nickel-63 in nickel und gamma-eisen, *Phys. Status Solidi* 5 (1) (1964) 63–71, <http://dx.doi.org/10.1002/pssb.19640050107>.
- [11] J.Q. Broughton, G.H. Gilmer, Harmonic analysis of Lennard-Jones fcc grain boundaries, *Modell. Simul. Mater. Sci. Eng.* 6 (4) (1998) 393–404, <http://dx.doi.org/10.1088/0965-0393/6/4/008>.
- [12] S.M. Foiles, Evaluation of harmonic methods for calculating the free-energy of defects in solids, *Phys. Rev. B* 49 (21) (1994) 14930–14938, <http://dx.doi.org/10.1103/PhysRevB.49.14930>.
- [13] S.M. Foiles, Temperature dependence of grain boundary free energy and elastic constants, *Scripta Mater.* 62 (5) (2010) 231–234, <http://dx.doi.org/10.1016/j.scriptamat.2009.11.003>.
- [14] R. Najafabadi, D.J. Srolovitz, R. Lesar, Thermodynamic and structural-properties of (001) twist boundaries in gold, *J. Mater. Res.* 6 (5) (1991) 999–1011, <http://dx.doi.org/10.1557/jmr.1991.0999>.
- [15] R. Najafabadi, H.Y. Wang, D.J. Srolovitz, R. Lesar, The effects of segregation on grain-boundary cohesive energies in Ni_{3-x}Al_{1+x}, *Scr. Metall. Mater.* 25 (11) (1991) 2497–2502, [http://dx.doi.org/10.1016/0956-716x\(91\)90056-7](http://dx.doi.org/10.1016/0956-716x(91)90056-7).
- [16] A.P. Sutton, Direct free-energy minimization methods – application to grain-boundaries, *Philos. Trans. R. Soc. Lond. Ser. A-Math. Phys. Eng. Sci.* 341 (1661) (1992) 233–245, <http://dx.doi.org/10.1098/rsta.1992.0097>.
- [17] C. Serre, P. Wynblatt, D. Chatain, Study of a wetting-related adsorption transition in the Ga–Pb system: 1. Surface energy measurements of Ga-rich liquids, *Surf. Sci.* 415 (3) (1998) 336–345, [http://dx.doi.org/10.1016/s0039-6028\(98\)00567-6](http://dx.doi.org/10.1016/s0039-6028(98)00567-6).
- [18] M.A. Gulgun, R. Voytovych, I. Maclaren, M. Ruhle, R.M. Cannon, Cation segregation in an oxide ceramic with low solubility: yttrium doped alpha-alumina, *Interface Sci.* 10 (1) (2002) 99–110, <http://dx.doi.org/10.1023/a:1015268232315>.
- [19] E.W. Hart, in: H. Hu (Ed.), *The Nature and Behavior of Grain Boundaries*, Plenum, New York, 1972, p. 155.
- [20] P. Wynblatt, D. Chatain, Solid-state wetting transitions at grain boundaries, *Mater. Sci. Eng. A-Struct. Mater. Prop. Microstruct. Process.* 495 (1–2) (2008) 119–125, <http://dx.doi.org/10.1016/j.msea.2007.09.091>.
- [21] S.A. Bojarski, M.P. Harmer, G.S. Rohrer, Influence of grain boundary energy on the nucleation of complexion transitions, *Scripta Mater.* 88 (1–4) (2014), <http://dx.doi.org/10.1016/j.scriptamat.2014.06.016>.
- [22] S.A. Bojarski, J. Knighting, S.L. Ma, W. Lenthe, M.P. Harmer, G.S. Rohrer, The relationship between grain boundary energy, grain boundary complexion transitions, and grain size in Ca-doped yttria, *Mater. Sci. Forum* 753 (2013) 87–92, <http://dx.doi.org/10.4028/www.scientific.net/MSF.753.87>.
- [23] S.A. Bojarski, S. Ma, W. Lenthe, M.P. Harmer, G.S. Rohrer, Changes in the grain boundary character and energy distributions resulting from a complexion transition in Ca-doped yttria, *Metall. Mater. Trans. A-Phys. Metall. Mater. Sci.* 43A (10) (2012) 3532–3538, <http://dx.doi.org/10.1007/s11661-012-1172-y>.
- [24] S.A. Bojarski, M. Stuer, Z. Zhao, P. Bowen, G.S. Rohrer, Influence of Y and La additions on grain growth and the grain-boundary character distribution of alumina, *J. Am. Ceram. Soc.* 97 (2) (2014) 622–630, <http://dx.doi.org/10.1111/jace.12669>.
- [25] S.J. Dillon, M.P. Harmer, G.S. Rohrer, The relative energies of normally and abnormally growing grain boundaries in alumina displaying different complexions, *J. Am. Ceram. Soc.* 93 (6) (2010) 1796–1802, <http://dx.doi.org/10.1111/j.1551-2916.2010.03642.x>.
- [26] S.J. Dillon, M.P. Harmer, G.S. Rohrer, Influence of interface energies on solute partitioning mechanisms in doped aluminas, *Acta Mater.* 58 (15) (2010) 5097–5108, <http://dx.doi.org/10.1016/j.actamat.2010.05.045>.
- [27] S.J. Dillon, H. Miller, M.P. Harmer, G.S. Rohrer, Grain boundary plane distributions in aluminas evolving by normal and abnormal grain growth and displaying different complexions, *Int. J. Mater. Res.* 101 (1) (2010) 50–56, <http://dx.doi.org/10.3139/146.110253>.
- [28] G.S. Rohrer, Grain boundary energy anisotropy: a review, *J. Mater. Sci.* 46 (18) (2011) 5881–5895, <http://dx.doi.org/10.1007/s10853-011-5677-3>.

- [29] W.W. Mullins, Theory of thermal grooving, *J. Appl. Phys.* 28 (3) (1957) 333–339.
- [30] C. Herring, Surface tension as a motivation for sintering, in: W.E. Kingston (Ed.), *The Physics of Powder Metallurgy*, McGraw-Hill, New York, 1951, pp. 143–179.
- [31] T. Sano, D.M. Saylor, G.S. Rohrer, Surface energy anisotropy of SrTiO₃ at 1400 °C in air, *J. Am. Ceram. Soc.* 86 (2003) 1933–1939.
- [32] D.M. Saylor, G.S. Rohrer, Measuring the influence of grain-boundary misorientation on thermal groove geometry in ceramic polycrystals, *J. Am. Ceram. Soc.* 82 (6) (1999) 1529–1536.
- [33] W. Robertson, Grain-boundary grooving by surface diffusion for finite surface slopes, *J. Appl. Phys.* 42 (1) (1971) 463, <http://dx.doi.org/10.1063/1.1659625>.
- [34] D.M. Saylor, D.E. Mason, G.S. Rohrer, Experimental method for determining surface energy anisotropy and its application to magnesia, *J. Am. Ceram. Soc.* 83 (5) (2000) 1226–1232.
- [35] D.M. Saylor, A. Morawiec, B.L. Adams, G.S. Rohrer, Misorientation dependence of the grain boundary energy in magnesia, *Interface Sci.* 8 (2–3) (2000) 131–140.
- [36] S.J. Dillon, M.P. Harmer, Direct observation of multilayer adsorption on alumina grain boundaries, *J. Am. Ceram. Soc.* 90 (3) (2007) 996–998, <http://dx.doi.org/10.1111/j.1551-2916.2007.01512.x>.
- [37] S.J. Dillon, M.P. Harmer, Multiple grain boundary transitions in ceramics: a case study of alumina, *Acta Mater.* 55 (15) (2007) 5247–5254, <http://dx.doi.org/10.1016/j.actamat.2007.04.051>.
- [38] S.J. Dillon, M.P. Harmer, Demystifying the role of sintering additives with complexion, *J. Eur. Ceram. Soc.* 28 (7) (2008) 1485–1493, <http://dx.doi.org/10.1016/j.jeurceramsoc.2007.12.018>.
- [39] W.E. Frazier, G.S. Rohrer, A.D. Rollett, Abnormal grain growth in the potts model incorporating grain boundary complexion transitions that increase the mobility of individual boundaries, *Acta Mater.* 96 (2015) 390–398, <http://dx.doi.org/10.1016/j.actamat.2015.06.033>.
- [40] T. Frolov, D.L. Olmsted, M. Asta, Y. Mishin, Structural phase transformations in metallic grain boundaries, *Nat. Commun.* 4 (2013), <http://dx.doi.org/10.1038/ncomms2919>.
- [41] T. Frolov, M. Asta, Y. Mishin, Segregation-induced phase transformations in grain boundaries, *Phys. Rev. B* 92 (2) (2015), <http://dx.doi.org/10.1103/PhysRevB.92.020103>.
- [42] Q. Gao, M. Widom, First-principles study of bismuth films at transition-metal grain boundaries, *Phys. Rev. B* 90 (14) (2014), <http://dx.doi.org/10.1103/PhysRevB.90.144102>.
- [43] C.S. Kim, A.D. Rollett, G.S. Rohrer, Grain boundary planes: new dimensions in the grain boundary character distribution, *Scripta Mater.* 54 (6) (2006) 1005–1009, <http://dx.doi.org/10.1016/j.scriptamat.2005.11.071>.
- [44] G. Rohrer, D. Saylor, B. El Dasher, B. Adams, A. Rollett, P. Wynblatt, The distribution of internal interfaces in polycrystals, *Zeitschrift Fur Metallkunde* 95 (4) (2004) 197–214.
- [45] H. Beladi, N.T. Nuhfer, G.S. Rohrer, The five-parameter grain boundary character and energy distributions of a fully austenitic high-manganese steel using three dimensional data, *Acta Mater.* 70 (2014) 281–289, <http://dx.doi.org/10.1016/j.actamat.2014.02.038>.
- [46] H. Beladi, G.S. Rohrer, The relative grain boundary area and energy distributions in a ferritic steel determined from three-dimensional electron backscatter diffraction maps, *Acta Mater.* 61 (4) (2013) 1404–1412, <http://dx.doi.org/10.1016/j.actamat.2012.11.017>.
- [47] D.M. Saylor, A. Morawiec, G.S. Rohrer, Distribution and energies of grain boundaries in magnesia as a function of five degrees of freedom, *J. Am. Ceram. Soc.* 85 (12) (2002) 3081–3083.
- [48] M. Tang, W.C. Carter, R.M. Cannon, Grain boundary order-disorder transitions, *J. Mater. Sci.* 41 (23) (2006) 7691–7695, <http://dx.doi.org/10.1007/s10853-006-0608-4>.
- [49] W.D. Kaplan, D. Chatain, P. Wynblatt, W.C. Carter, A review of wetting versus adsorption, complexions, and related phenomena: the rosetta stone of wetting, *J. Mater. Sci.* 48 (17) (2013) 5681–5717, <http://dx.doi.org/10.1007/s10853-013-7462-y>.
- [50] J. Luo, Stabilization of nanoscale quasi-liquid interfacial films in inorganic materials: a review and critical assessment, *Crit. Rev. Solid State Mater. Sci.* 32 (1–2) (2007) 67–109, <http://dx.doi.org/10.1080/10408430701364388>.
- [51] G.S. Rohrer, M. Affatigato, M. Backhaus, R.K. Bordia, H.M. Chan, S. Curtarolo, A. Demkov, J.N. Eckstein, K.T. Faber, J.E. Garay, Y. Gogotsi, L.P. Huang, L.E. Jones, S. V. Kalinin, R.J. Lad, C.G. Levi, J. Levy, J.P. Maria, L. Mattos, A. Navrotsky, N. Orlovskaya, C. Pantano, J.F. Stebbins, T.S. Sudarshan, T. Tani, K.S. Weil, Challenges in ceramic science: a report from the workshop on emerging research areas in ceramic science, *J. Am. Ceram. Soc.* 95 (12) (2012) 3699–3712, <http://dx.doi.org/10.1111/jace.12033>.
- [52] I.M. Robertson, C.A. Schuh, J.S. Vetrano, N.D. Browning, D.P. Field, D.J. Jensen, M. K. Miller, I. Baker, D.C. Dunand, R. Dunin-Borkowski, B. Kabius, T. Kelly, S. Lozano-Perez, A. Misra, G.S. Rohrer, A.D. Rollett, M.L. Taheri, G.B. Thompson, M. Uchic, X.-L. Wang, G. Was, Towards an integrated materials characterization toolbox, *J. Mater. Res.* 26 (11) (2011) 1341–1383, <http://dx.doi.org/10.1557/jmr.2011.41>.
- [53] N. Zhou, J. Luo, Developing grain boundary diagrams for multicomponent alloys, *Acta Mater.* 91 (2015) 202–216, <http://dx.doi.org/10.1016/j.actamat.2015.03.013>.
- [54] P.R. Cantwell, S. Ma, S.A. Bojarski, G.S. Rohrer, M.P. Harmer, Expanding time-temperature-transformation (TTT) diagrams to interfaces: a new approach for grain boundary engineering, *Acta Mater.* 106 (2016) 78–86, <http://dx.doi.org/10.1016/j.actamat.2016.01.010>.